Azo-Containing Polymers with Degradation On-Demand Feature

Mathieu A. Ayer[1], Yoan C. Simon[1,2], Christoph Weder[1]*

[1]Adolphe Merkle Institute, University of Fribourg, Chemin des Verdiers 4, 1700 Fribourg, Switzerland

[2]School of Polymers and High Performance Materials, The University of Southern Mississippi, 118 College Dr., Hattiesburg MS 39406, USA

ABSTRACT. Molecules comprising aliphatic azo moieties are widely used as radical polymerization initiators, but only few studies have explored their usefulness as stimuli-responsive motifs in macromolecular constructs. The controlled degradation of azo-containing polymers has indeed remained largely unexplored. Here we present the syntheses of linear azo-containing polyamides and polyurethanes and report on their thermally and optically induced responses in solution and the solid state. We show that the stimuli-induced degradation behavior depends strongly on the nature of the polymer backbone, the state of matter, and in solution, on the nature of the solvent. The stimuli-responsive solid-state properties of the azo-containing materials may be particularly useful. In the case of the polyurethanes studied here, temperature- or light-induced cleavage of the azo motifs led to a controllable decrease of the molecular weight, which in turn caused a reduction of the elongation at break, modulus and strength. The controlled degradation of the polymer in well-defined areas can be readily achieved via photopatterning, and this approach was shown to be useful to produce solid structures with graded mechanical properties.

INTRODUCTION

Polymers which can be degraded on command, i.e., upon exposure to a pre-defined external stimulus, are of great interest in the context of recycling,[1] debonding-on-demand adhesives,[2] small molecules release,[3] biomedical applications,[1] sensors,[4] and many other applications.[5,6] To achieve degradability, a variety of concepts have been investigated, including the introduction of chemically labile groups (such as esters or acetals),[7] the design of self-immolative polymers (which undergo depolymerization upon cleavage of stimuli-responsive end-groups),[8] the stimuli-driven disassembly of supramolecular polymers,[2] the (dis)assembly of nanoparticles based on polymers exhibiting a lower critical solution temperature (LCST),[9] and the introduction of stimuli-responsive moieties that can be preferentially cleaved upon exposure to a specific stimulus or a combination thereof.[1,10] In addition to hydrolyzable or biodegradable motifs resulting from polycondensation,[1,7] the introduction of specific light- and heat-sensitive "weak links" has been broadly explored, e.g. spiropyrans, phtalaldehydes, disulfides, Diels-Alder products, and *o*-nitrobenzyl ester or ether motifs.[1,8,10,11] Remarkably, the degradation characteristics of most of these systems were studied in solution, while examples of controlled light or heat triggered degradation in the solid have been less frequently explored[11,12] or involved a solid-liquid interface.[13] In many cases, the degradation process involves a depolymerization reaction.[8] Interestingly, azo motifs, which are extensively used as radical polymerization initiators, have not been used in the context of controlled polymer degradation. These motifs are however well known to dissociate upon heating, exposure to light, and ultrasonication, and have previously been incorporated into various polymers. The latter were used as radical macroinitiators for the synthesis of well-defined block copolymers,[14-21] the fabrication of cross-linked PMMA microspheres,[22] and for the release of molecules grafted onto nanoparticles in

imaging or delivery applications.[23,24] It was also shown that the azo-motif can be used to create mechanoresponsive materials that can be degraded upon ultrasonication in solution.[25] We show here that polyamides and polyurethanes comprising 4,4′ -azobis(4-cyanovaleric acid) or 2,2'-azobis[2-methyl-N-(2-hydroxyethyl)propionamide] residues in the backbone display mechanical characteristics that are virtually identical to those of the azo-free reference materials. However, these materials can be degraded "on command" upon heating or exposure to (ultraviolet) light. Interestingly, the stimulus-induced degradation behavior of the two azo-motif containing polymers shows significant differences, which highlight the importance of minor design variations.

EXPERIMENTAL SECTION

Materials. Anhydrous *N*-methyl-2-pyrrolidone (NMP, Sigma-Aldrich) was used as solvent for the synthesis of the polyamides. Fresh inhibitor-free anhydrous tetrahydrofuran (THF) (Sigma-Aldrich) was utilized as solvent for the synthesis of the polyurethanes and film casting. Stabilized anhydrous THF (Sigma-Aldrich) was employed for controlled degradation experiments taking place in solution. Jeffamine ED-2003 (JA, number-average molecular weight, M_n=2,000 g/mol), kindly provided by Huntsman Corp., and 1,10-diaminodecane (DAD) were dried in vacuo overnight prior to use. Poly(tetrahydrofuran) (PTHF, M_n=2,000 g/mol) was dried in vacuo at 100 °C for 1 h prior to reaction. 4,4'-Methylenebis(phenyl isocyanate) (MDI) and 1,4-butanediol (BDO) were distilled under vacuum and stored over molecular sieves at 5 °C. 4,4'-Azobis(4-cyanovaleric chloride) (ACVC, **1**) was synthesized by adapting procedures described in the literature.[20,21] 2,2'-Azobis[2-methyl-N-(2-hydroxyethyl)propionamide] (**2**) was generously donated by Wako Pure Chemicals Industries, Ltd. (VA-086). Compound **2** was dried

in vacuo at rt overnight prior to reaction. All other reagents were purchased from Sigma-Aldrich and used as received.

Instrumentation. ^{1}H NMR and ^{13}C NMR spectra were recorded on Bruker Avance III or Avance III HD spectrometers at 300 or 400 MHz (^{1}H) and 75 or 100 MHz (^{13}C), respectively. The chemical shifts (δ) are reported in parts per million (ppm,) relative to tetramethylsilane, although referencing was based on residual solvent protons. Size exclusion chromatography (SEC) measurements were carried out on an Agilent Technologies 1200 system equipped with a Wyatt Optilab rEX differential refractive index (dRI) detector and a Wyatt miniDAWN TREOS multi-angle laser light scattering (MALLS) detector. The column system was composed of an a Agilent 5 μm MIXED-C guard column and either a PLgel 5 μm MIXED-C (200-2,000,000 g/mol) column or a 5 μm MIXED-D (200-400,000 g/mol) column from Agilent. THF was employed as solvent/eluent and the measurements were carried out at a flow rate of 1 mL/min. The mass-average molecular weight (M_w) and M_n values were determined in comparison with polystyrene standards. Thermogravimetric analysis (TGA) measurements were carried out under N_2 with a Mettler-Toledo Star^e system by heating from 25 °C to 500 °C at a rate of 10 °C/min. Differential scanning calorimetry (DSC) measurements were carried out under N_2 on Mettler-Toledo Star^e DSC or DSC 2 systems at heating and cooling rates of 10 °C/min. Elemental analyses (EA) were performed on a CE Instruments EA 1110 by flash combustion and GC separation. Fourier transform infrared (FT-IR) spectra were recorded on a PerkinElmer Spectrum 65 spectrometer equipped with an attenuated total reflection (ATR) accessory. Ultraviolet-visible (UV-Vis) spectra were measured on a Shimadzu UV-2401PC spectrophotometer. Dynamic mechanical analyses (DMA) were carried out under N_2 on a TA Instruments DMA Q800 at a heating rate of 3 °C/min, a frequency of 1 Hz and an amplitude of 15 μm. Stress-strain

measurements were performed under ambient conditions with a Zwick/Roell Z010 tensile tester mounted with a 200 N load cell at a strain rate of 150 mm/min, using dogbone-shaped specimens (total length: 75 mm; cross-section: 4.1 mm; length of measured part: 30 mm) that were cut from polymer films with a Zwick/Roell ZCP 020 manual cutting press mounted with the corresponding mold.

Synthesis of 4,4′ -azobis(4-cyanovaleric chloride) (ACVC, 1). In a dried two-neck 100 mL round-bottomed flask connected to a trap containing a concentrated aqueous NaOH solution and an N_2 inlet, 4,4′ -azobis(4-cyanovaleric acid) (ACVA, 1.50 g, 4.73 mmol) was dissolved in thionyl chloride (15 mL) at 0 °C under magnetic stirring. The reaction mixture was allowed to warm to rt and was stirred under a continuous flow of N_2 for 4 h, before an additional portion of thionyl chloride (5 mL) was added. The reaction mixture was stirred overnight at rt under N_2. At this point, all of the thionyl chloride had evaporated, and the residue was dissolved in chloroform (3 mL) and slowly pipetted into cold pentane (300 mL). The resulting precipitate was collected by filtration. To remove unreacted **1**, the residue was dissolved in dichloromethane (DCM, 2 mL), the solution was filtered and the solvent was evaporated. After drying in vacuo, **1** (1.124 g, 75% yield) was obtained as a pale yellow powder. ^{1}H NMR ($CDCl_3$, 300 MHz): δ = 3.24-2.90 (m, 4H, CH_2-COCl), 2.66-2.41 (m, 4H, CH_2), 1.73 (d, 6H, CH_3).

Synthesis of polyamides. Azo-PA was prepared as follows: In a dried two-neck 50 mL round-bottomed flask equipped with septa, JA (M_n=2,000 g/mol, 1.603 g, 0.802 mmol) and DAD (0.035 g, 0.200 mmol) were dissolved in NMP (10 mL) under N_2 atmosphere. The clear solution was cooled to 0 °C, propylene oxide (PO, HCl scavenger, 0.249 g, 4.3 mmol), sebacoyl chloride (SC, 0.191 g, 0.797 mmol) and **1** (0.064 g, 0.202 mmol) were added. After stirring for 30 min, the cooling bath was removed and the reaction was allowed to proceed at rt under constant ma-

gnetic agitation. After 4 days, the clear reaction mixture was slowly precipitated into cold diethyl ether (400 mL) and the white precipitate that formed was collected by filtration and finally dried in vacuo overnight. **Azo-PA** was obtained as a pale yellow solid (1.285 g, 68%). ^{1}H NMR ($CDCl_3$, 400 MHz): δ = JA residue: 4.10 (m, 2H, CH-NH), 3.81 (d, 4H, CH_2), 3.80 (d, 4H, CH_2), 3.68-3.35 (m, CH_2/CH, obstructed), 3.63 (s, 4H, CH_2), 1.29 (s, 3H, CH_3); DAD residue: 3.22 (q, 4H, CH_2-CO), 1.48 (quint, 4H, CH_2), 1.17-1.08 (m, 14H, CH_2, obstructed); SC residue: 2.15 (t, 4H, CH_2-CO), 1.60 (quint, 4H, CH_2), 1.17-1.08 (m, 8H, CH_2, obstructed); **1** residue: 2.46-2.25 (m, 4H, CH_2, obstructed), 2.10-2.00 (m, 4H, CH_2, obstructed); 1.70 (d, 6H, CH_3). Amides: 6.26 (s, 1H, NH), 5.96 (s, 1H, NH). End groups: 5.09 (m, 1H, CH-NH_2), 3.35 (t, 2H, CH_2-CO). ^{13}C NMR ($CDCl_3$, 100 MHz): δ = 172.75, 75.53, 75.33, 75.17, 73.39, 72.40, 72.09, 70.88, 70.70, 45.42, 45.26, 36.93, 29.37, 29.25, 25.88, 17.97, 17.89, 17.39, 17.30, 17.19, 17.10). Anal. Calcd for $(JA_{0.802}DAD_{0.200}SC_{0.797}\mathbf{1}_{0.202})_n$: C, 57.03; H, 9.41; N, 2.04. Found: C, 56.5; H, 9.8; N, 2.0.

Ref-PA was synthesized using the same procedure, but **1** was omitted and the following quantities were used: JA (1.604 g, 0.802 mmol), DAD (0.036 g, 0.209 mmol), NMP (10 mL), PO (0.249 g, 4.287 mmol), SC (0.247 g, 1.031 mmol). **Ref-PA** was obtained as a white solid (1.607 g, 85%). ^{1}H NMR ($CDCl_3$, 400 MHz): δ = JA residue: 4.09 (m, 2H, CH-NH), 3.81 (d, 4H, CH_2), 3.79 (d, 4H, CH_2), 3.68-3.35 (m, CH_2/CH, obstructed), 3.63 (s, 4H, CH_2), 1.28 (s, 3H, CH_3); DAD residue: 3.22 (q, 4H, CH_2-CO), 1.49 (quint, 4H, CH_2), 1.17-1.08 (m, 14H, CH_2, obstructed); SC residue: 2.13 (t, 4H, CH_2-CO), 1.60 (quint, 4H, CH_2), 1.17-1.08 (m, 8H, CH_2, obstructed); Amides: 6.30 (s, 1H, NH), 6.02 (s, 1H, NH). End groups: 5.09 (m, 1H, CH-NH_2), 3.35 (t, 2H, CH_2-CO, obstructed). ^{13}C NMR ($CDCl_3$, 100 MHz): 172.97, 75.51, 75.31, 72.31, 72.04, 70.69, 45.51, 45.34, 36.80, 29.32, 29.09, 25.88, 17.82, 17.27, 17.15. Anal. Calcd for $(JA_{0.802}DAD_{0.209}SC_{1.031})_n$: C, 57.30; H, 9.51; N, 1.47. Found: C, 56.2; H, 9.9; N, 1.4

Synthesis of polyurethanes. Azo-PU was prepared as follows: In a dried two-neck 100 mL round-bottomed flask equipped with septa, PTHF (M_n=2000 g/mol, 4.214 g, 2.107 mmol) and **2** (0.346 g, 1.200 mmol) were stirred in THF (20 mL) under N_2 to afford a white dispersion. BDO (0.356 g, 3.950 mmol) was then added dropwise with a syringe. A solution of MDI (1.991 g, 7.957 mmol, NCO/OH molar ratio ca. 1.10) in THF (10 mL) was rapidly added with a syringe. Finally, dibutyltin dilaurate (DBTDL, 3 drops) was added with a syringe and the homogeneous reaction mixture was stirred at rt for 48 h. At this time, FT-IR analysis revealed the disappearance of the NCO signals at 2282 cm^{-1}, and the polymer was precipitated into EtOH (2x800 mL). The resulting precipitate was collected by filtration and dried in vacuo. **Azo-PU** was obtained as a white fibrous, rubbery solid (5.823 g, 84%). ^{1}H NMR (THF-d_8, 400 MHz): δ = MDI residue: 9.57 (s, 2H, NH), 9.55 (s, 2H, NH), 7.36 (d, 4H, ArH), 7.04 (d, 4H, ArH), 3.82 (s, 2H, CH_2-Ar); PTHF residue: 4.10 (t, 4H, CH_2-OOC), 3.37 (s, 108H, CH_2-O), 1.69 (s, 4H, CH_2), 1.59 (s, 108H, CH_2); BDO residue: 4.13 (d, 4H, CH_2-O), 1.73 (4H, CH_2 obstructed); **2** residue: 8.69 (s, 2H, NH), 7.30 (s, 2H, NH), 4.16 (t, 4H, CH_2-OOC), 3.48 (q, 4H, CH_2-NH), 1.33 (s, 12H, CH_3); end groups: 6.82 (d, 2H, ArH), 6.47 (d, 2H, ArH), 4.65 (s, 2H, NH_2). ^{13}C NMR (THF-d_8, 100 MHz): δ = 173.94 (**2** residue), 154.37, 138.73, 138.64, 136.43, 136.33, 129.87 (**2**), 129.83, 119.15, 118.97, 75.72 (**2**), 71.45, 71.38, 71.01, 65.01, 64.75, 63.66 (**2**), 41.32, 40.12 (**2**), 27.70, 27.35, 27.10, 26.80, 23.39 (**2**). Anal. Calcd for $(MDI_{7.957}BDO_{3.950}PTHF_{2.107}\mathbf{2}_{1.200})_n$: C, 66.29; H, 8.98; N, 4.20. Found: C, 65.62; 9.25; N, 3.88.

Ref-PU was synthesized using the same procedure, but **2** was omitted and the reaction was conducted at a larger scale, using the following quantities: PTHF (9.994 g, 4.997 mmol), BDO (0.837 g, 9.284 mmol), MDI (3.945 g, 15.765 mmol), DBTDL (4 drops). **Ref-PU** was obtained as a white fibrous, rubbery solid (13.298 g, 90%). ^{1}H NMR (THF-d_8, 400 MHz): δ = MDI

residue: 9.57 (s, 2H, NH), 9.54 (s, 2H, NH), 7.36 (d, 4H, ArH), 7.03 (d, 4H, ArH), 3.82 (s, 2H, CH_2-Ar); PTHF residue: 4.09 (t, 4H, CH_2-OOC), 3.37 (s, 108H, CH_2-O), 1.69 (s, 4H, CH_2), 1.58 (s, 108H, CH_2); BDO residue: 4.13 (d, 4H, CH_2-O), 1.73 (4H, CH_2 obstructed); end groups: 6.82 (d, 2H ArH), 6.47 (d, 2H ArH), 4.65 (s, 2H, NH_2). ^{13}C NMR (THF-d_8, 100 MHz): δ = 154.37, 138.73, 138.64, 136.43, 136.33, 129.83, 119.15, 118.97, 71.45, 71.38, 71.01, 65.00, 64.75, 41.32, 27.70, 27.35, 27.10, 26.80. Anal. Calcd for $(MDI_{15.765}BDO_{9.284}PTHF_{4.997})_n$: C, 66.90; H, 9.27; N, 2.99. Found: C, 66.33; 9.53; N, 2.87.

Polymer film preparation. For films with a diameter of 6.5 cm, solutions of the various polymers (ca. 0.5 g) in THF (10 mL) were cast into round 25 mL poly(tetrafluoroethylene) (PTFE) Petri dishes (65x12 mm), which were subsequently placed in a well-ventilated hood under an inverted funnel that was used to control the evaporation rate of the solvent so that the films dried overnight under ambient conditions. Drying was completed in vacuo at rt overnight and transparent films with a thickness of ca. 110-120 μm were obtained of all polymers. Films thus prepared were used for the characterization of physical properties (TGA, DSC, EA, UV-Vis, DMA) and for controlled degradation experiments in the solid state. Films with a diameter of 10 cm were produced by the same process, but using ca. 1.5 g of the polymer, 30 mL THF, and a larger Petri dish (102x20 mm). These samples, which also had a thickness of ca. 110-120 μm, were cut into dogbone-shaped specimens (total length: 75 mm; cross-section: 4.1 mm; length of measured part: 30 mm) that were used for stress-strain measurements. The sample used in Figure 6 had a thickness of 180 μm.

Controlled degradation by heat or light treatment. Before any degradation experiments either in solution or solid state, the polymer film samples were dried in vacuo at rt for at least 1 h. For degradation experiments carried out in solution, 2 or 5 mL pressure-withstanding

microwave vials were used and a small amount of polymer film (ca. 5-10 mg) was dissolved in the desired solvent at a concentration of 2.5 mg/mL, before the vial was sealed and rapidly heated to the desired temperature (140-160 °C), reached and probed precisely using a Biotage Initiator 2.5 microwave synthesizer. These temperatures were achievable under formation of a light pressure (ca. 3 bar). After maintaining this temperature for 5 min, the solution was cooled to rt, the solvent was removed in vacuo overnight, and the residue was dissolved in THF for SEC analysis. For heat-induced degradation experiments carried out in the solid state, the samples were placed in a Carver CE Press that had been preheated to the desired temperature (140-160 °C) under very light pressure between two PTFE sheets and kept in the press for the desired time (5-10 min). Irradiation of the polymer films with UV light was done with a Hönle Bluepoint 4 Ecocure UV lamp equipped with an optical fiber and a 320-390 nm filter; the power density was 600 mW/cm^2 and the distance between the optical fiber and the sample was kept at 15 mm. UV light treatments in solution were applied to polymer solutions (1 mL vial, 2.5 mg/mL) under the same conditions. Irradiation of solid-state samples with visible light involved the same setup, but a 390-500 nm filter was used and the fiber-sample distance was increased to 35 mm. In this particular case, the emission spectrum was measured with an Ocean Optics USB4000 spectrometer and the surface temperature of the films during irradiation experiments was monitored using an Optris PI 160 infrared camera.

The temperature- and light-induced changes to the polymers in the solid state were studied by SEC, ^{1}H NMR spectroscopy, and EA. The SEC measurements were performed after dissolving the samples in THF (2.5 mg/mL) following the respective treatment. The ^{1}H NMR spectra were recorded after application of a thermal stimulus (exposure to 140 °C for 5 min in the case of the PAs and 150 °C for 5 min and 30 min in the case of the PUs) and subsequent dissolution in

deuterated solvent. The EA measurements were carried out several hours after heating (140 °C for 5 min for the PAs and 150 °C for 5 min for the PUs).

RESULTS AND DISCUSSION

Design of materials, synthesis, characterization

4,4′ -Azobis(4-cyanovaleric chloride) (**1**) and 2,2'-azobis[2-methyl-N-(2-hydroxyethyl)-propionamide] (**2**) were used here as potentially degradable monomers in the syntheses of polyamides (PAs) and polyurethanes (PUs), respectively (Scheme 1). These azo-compounds are widely used as initiators in radical polymerization reactions, which exploit that upon homolytic dissociation of the C-N bonds, N_2 is released and two carbon-centered radicals are formed, which serve as the chain-initiating species. Azo compounds such as **1** and **2** display rather low thermal dissociation energies (of the order of 130 – 150 kJ/mol), which translate into 10 h half-life temperatures of 69 °C for the diacid precursor of **1** and of 86 °C for **2** (measured in aqueous solutions).[26] We speculated that the thermal stability of these motifs might be sufficiently high to allow for the synthesis and processing of the targeted polymers, but low enough to permit controlled degradation by way of selective cleavage of the azo-motifs vs. all other bonds comprised in the polymer backbones. The presence of peripheral functional groups, i.e., carboxylic acid chlorides and alcohols in the case of **1** and **2**, respectively, permits the incorporation of these azo compounds into the backbone of the targeted polymers. We note that the choice of the substituents on the carbon atoms adjacent to the N=N bond (i.e. methyl, methylene and nitrile in the case of **1** and two methyl and an amide in the case of **2**) influences the stability of the resulting radicals; thus the dissociation energy and temperature can readily be tuned within substantial ranges.[27,28] Moreover, certain azo motifs, including the ones utilized

here, can also be photolytically cleaved, as they absorb in the near UV range due to the Q → N transition resulting from the approximate sp^3 hybridization of the nitrogen lone electron pair orbital. The subsequent homolytic C-N bond cleavage occurs either due to a simultaneous dissociation of both bonds of the excited state molecule or through the decomposition of the very unstable RN_2· radical intermediate.[27,29,30] Thus, **1** and **2** should be useful for the design of thermally as well as optically degradable polymers.

We elected to synthesize and explore an azo-motif containing polyamide (**azo-PA**) as well as a corresponding polyurethane (**azo-PU**), both with a segmented structure composed of hard and soft segments, with the goal of creating materials that exhibit a high toughness, and which would retain some mechanical integrity after dissociation of (some of) the azo motifs comprised in the macromolecules. As this requires a number-average molecular weight (M_n) of the order of 15,000-20,000 g/mol, we limited the fraction of azo compounds **1** and **2** in the feed to 10 mol% (corresponding to 3.5% w/w) in the case of the **azo-PA** and 8 mol% (corresponding to 5% w/w) in the case of the **azo-PU**. For reference purposes, the corresponding polymers without azo moieties were also synthesized (**ref-PA** and **ref-PU**). Hard blocks, providing physical cross-links, were composed of H-bonding amides formed by the reaction of 1,10-diaminodecane (DAD) and sebacoyl chloride (SC) in the case of the PAs, and of urethanes resulting from the reaction of butane diol (BDO) and 4,4'-methylenebis(phenyl isocyanate) (MDI) in the case of the PUs, while an amine-terminated poly(propylene glycol-*block*-ethylene glycol-*block*-propylene glycol) telechelic (Jeffamine, JA) and telechelic poly(tetrahydrofuran) (PTHF), were used as soft blocks for the PAs and PUs, respectively. Interestingly, as will be discussed later, the two polymer families exhibit different thermal dissociation characteristics depending on the azo motifs they contain.

Scheme 1. Synthesis of the azo-group containing polyamide azo-PA and polyurethane azo-PU and the corresponding azo-free reference polymers ref-PA and ref-PU.

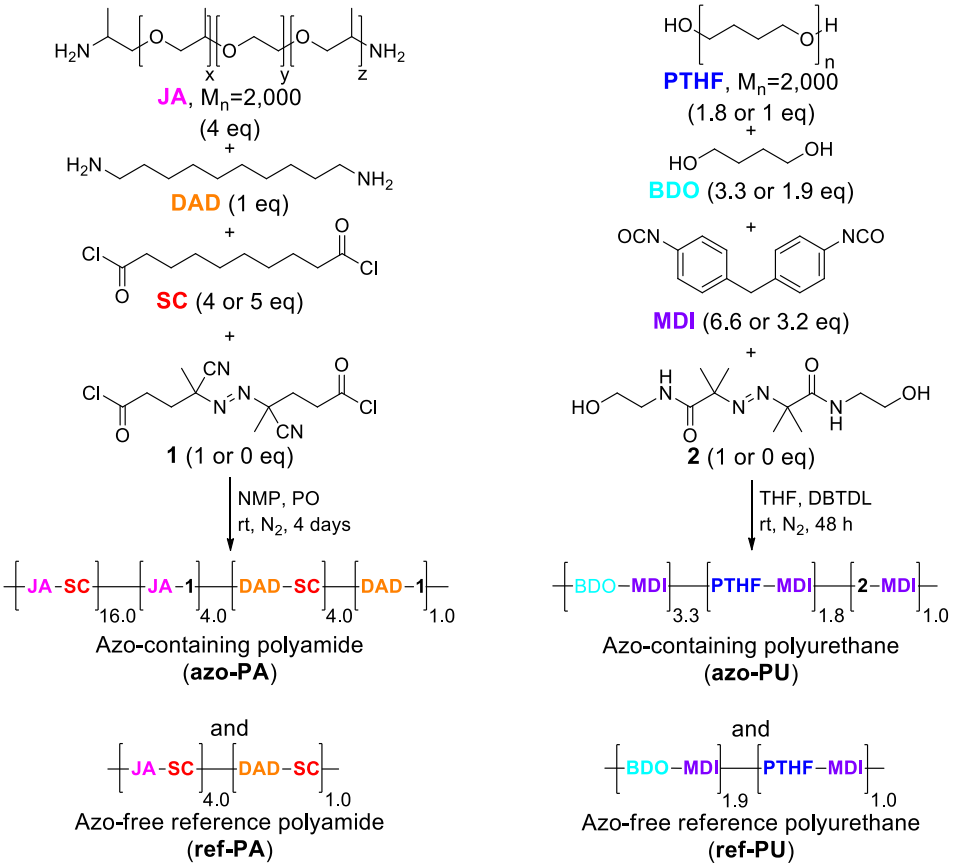

The polyamides **azo-PA** and **ref-PA** were synthesized by the low-temperature solution polycondensation reaction of DAD, JA (M_n=2,000 g/mol), SC and (in the case of the **azo-PA**) **1** in NMP (Scheme 1a).[31] Propylene oxide was used to neutralize the HCl released during the polycondensation, giving easily removable volatiles,[32] and an equimolar ratio of hard and soft segments was used. The polyurethanes **azo-PU** and **ref-PU** were synthesized using an established protocol[33] by reacting MDI with BDO, PTHF (M_n=2,000 g/mol) and (in the case of the **azo-PU**) **2** in THF, using dibutyltin dilaurate (DBTDL) as catalyst (Scheme 1b); a slight excess of MDI (NCO/OH ratio of 1.10) was necessary to obtain polymers with satisfactory molecular weight. All polymers made were recovered by precipitation and filtration and were

characterized to satisfaction by FT-IR, ^{1}H and ^{13}C NMR spectroscopy and elemental analysis (Supporting Information, Figures S1-S18). The molecular weights, determined by size exclusion

Table 1. General parameters of the azo-containing polyamide and polyurethane (azo-PA and azo-PU) and the corresponding azo-free control polymers (ref-PA, ref-PU) synthesized.

	molar ratio of monomers in feed[a]				weight fraction of azo motif in					
	JA	DAD	**1**	SC	**feed**	**polymer**[b]	**HS/SS**[c]	M_n[d] **(g/mol)**	$Đ$[d]	T_g[e] **(°C)**
Azo-PA	0.802	0.200	0.202	0.797	3.4	3.4	1:1	23,400	1.41	-15 ± 2
Ref-PA	0.802	0.209	0	1.031	0	0	1:1	24,700	1.67	-21 ± 1
	PTHF	BDO	**2**	MDI						
Azo-PU	2.107	3.950	1.200	7.957	5.0	4.9	1.2:1	49,300	1.90	-38 ± 4
Ref-PU	4.997	9.284	0	15.765	0	0	1.9:1	93,600	2.19	-41 ± 2

[a]JA=Jeffamine; DAD=diaminodecane; SC=sebacoyl chloride; PTHF=poly(tetrahydrofuran); BDO=butanediol; MDI=4,4'-methylenebis(phenyl isocyanate). [b]Determined by ^{1}H NMR spectroscopy. [c]Molar ratio of hard and soft segments. [d]Number-average molecular weight and dispersity, determined by size exclusion chromatography (SEC). [e]Determined by dynamic mechanical analysis (DMA).

chromatography (SEC), and the reactions parameters are compiled in Table 1. Gratifyingly, both azo-motif-containing polymers have appreciable M_n values (ca. 23,400 g/mol in the case of the **azo-PA** and 49,300 g/mol in the case of the **azo-PU**) and typical dispersity values $Đ$ (ca. 1.5 in the case of the PAs and ca. 2 in the case of the PUs). By and large, the data of the azo-free reference polymers are comparable to those of the azo-containing polymers, although in the case of the **ref-PU** a significantly higher M_n value was observed. A comparison of the ^{1}H NMR signals associated with the methyl protons of the residues of **1** (1.69 ppm) and **2** (1.33 ppm) (Supporting Information, Figures S3 and S11, Table 1) and methylene protons of the residues of DAD (3.22 ppm, alpha to carbonyl) and MDI (3.82), respectively, reveals that the concentrations of the azo-containing moieties in the polymers are comparable to those in the monomer feeds. This result is further confirmed by elemental analyses, which reveal higher nitrogen contents for

the azo-containing polymers in comparison to the azo-free reference materials (Supporting Information). Thus, all analytical data confirm the successful outcome of the polymerization reactions, the absence of any adverse effects associated with the azo motifs, and the quantitative integration of the azo-motifs into the polymer backbones.

Thermal and mechanical properties

Thermogravimetric analyses (TGA) reveal that a thermal window in which the azo motifs are stable is available below ca. 90 °C for the **azo-PA** and 120 °C for the **azo-PU** for the processing of the polymers (Figures 1a and 2a), although we note that these limiting temperatures depend on the heating rate. Above these thresholds, both TGA traces display a step-wise weight loss that is not seen in the TGA traces of the corresponding azo-free reference polymers (Supporting Information, Figures S19 and S20) and appears to indicate the loss of N_2 upon decomposition (Figures 1a and 2a). Indeed, a weight reduction of the order of 1% matches the weight reduction expected from the loss of all N_2 contained in **azo-PA** and **azo-PU**, i.e. the N=N motif corresponding to ca. 10 wt% of the azo compounds **1** and **2**. However, the thermal degradation profiles are not clear-cut "steps"; in both cases the TGA traces have a slightly negative slope, indicating further decomposition, until significant rate changes at ca. 350 °C (**azo-PA)** and 250 °C and 300 °C (**azo-PU**) reveal decomposition processes that are also seen in the TGA traces of the azo-free reference polymers (Supporting Information, Figures S19 and S20).

The differential scanning calorimetry (DSC) first heating trace of **azo-PA** shows a sharp endothermic transition at 37 °C, which is associated with the melting of the crystalline fraction, and a broad exothermic transition that stretches from 100 to 150 °C, which is neither present in the second heating scan nor in the DSC traces of **ref-PA** and thus appears to reflect the decomposition of the azo motif (Figure 1b, Supporting Information, Figures S21a and S22a).

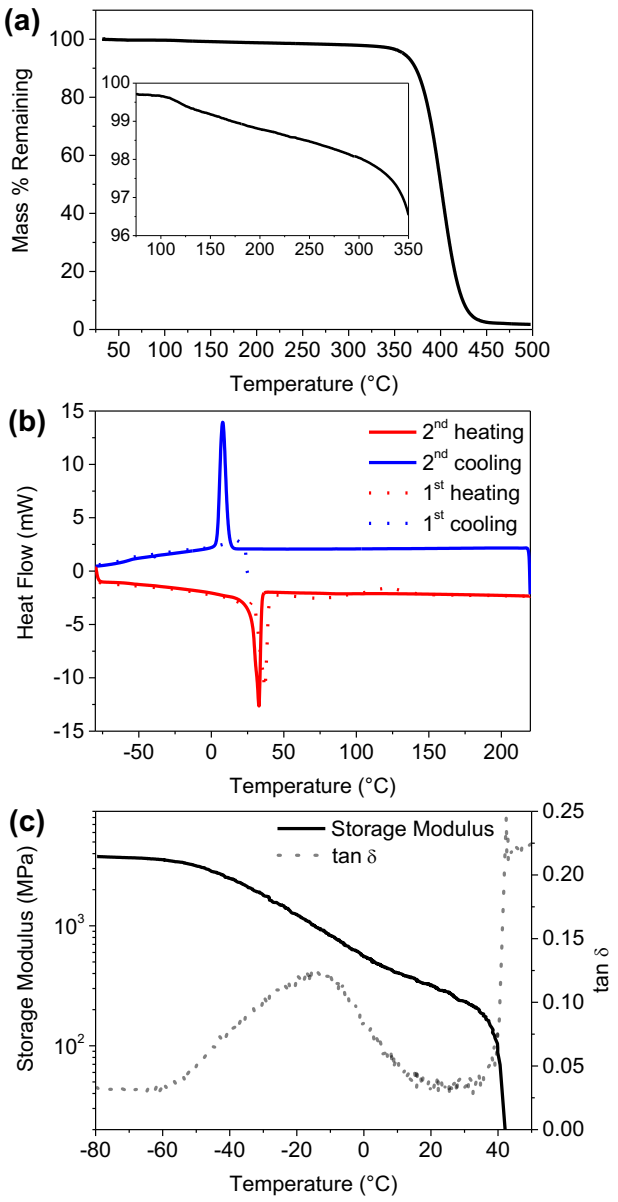

Figure 1. Thermal and thermomechanical properties of the azo-containing polyamide (**azo-PA**). (a) Thermogravimetric analysis (TGA) trace. (b) Differential scanning calorimetry (DSC) trace. (c) Dynamic mechanical analysis (DMA) data. All experiments were conducted under N_2 at heating/cooling rates of 10 ºC/min (TGA, DSC) or 3 ºC/min (DMA).

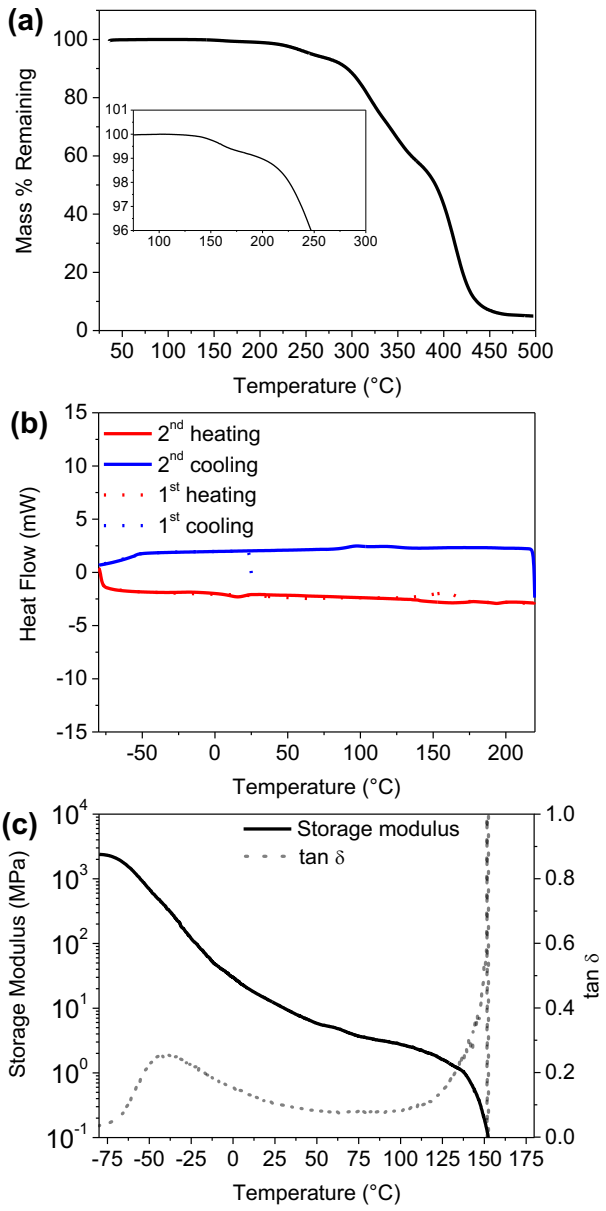

Figure 2. Thermal and thermomechanical properties of the azo-containing polyurethane (**azo-PU**). (a) Thermogravimetric analysis (TGA) trace. (b) Differential scanning calorimetry (DSC) trace. (c) Dynamic mechanical analysis (DMA) data. All experiments were conducted under N_2 at heating/cooling rates of 10 ºC/min (TGA, DSC) or 3 ºC/min (DMA).

Cooling and second heating traces of the **azo-PA** show exclusively sharp peaks around 9 °C (cooling, exothermic) and 33 °C (heating, endothermic) related to the crystallization and melting. The melting temperature (T_m) recorded upon second heating of **azo-PA** is slightly lower than the one observed for the pristine material, but it matches the values observed for the **ref-PA** (first and second heating) and **azo-PA** that had been heated to 60 °C only (Supporting Information, Figure S21b and 22b). In summary, the DSC data reveal the semicrystalline nature of the PAs, show that the melting temperature of the crystalline portion is slightly reduced upon decomposition of the azo motif, and that such decomposition can be suppressed if the temperature is kept below ca. 60 °C.

The DSC first heating trace of the **azo-PU** displays only a weak, irreversible, broad exothermic transition between 140 and 170 °C that is absent in the second heating scan and the DSC traces of the **ref-PU** and thus interpreted as dissociation of the azo motif, whereas the second heating scans - and in the case of the **ref-PU** also the first heating scan - shows only a weak exothermic transition around 175 °C, that reflects the melting of the PU's hard segments (Figure 2b, Supporting Information, Figures S23 and S24).

Dynamic mechanical analyses (DMA) were carried out to gain an overview of the thermo-mechanical properties of the polymers studied. The DMA traces of **azo-PA** and **ref-PA** are virtually identical; they reveal a rigid regime with a tensile storage modulus (*E*') of ca. 3.7 GPa below -60 °C, an extremely broad glass transition that extends from -55 to 20 °C and features a maximum at -15 °C (**azo-PA**) and -21 °C **ref-PA** (Figure 1c, Supporting Information, Figure S25). Both materials display a room-temperature (25 °C) *E*' of ca. 250 MPa, and fail around 40 °C, i.e., around the T_m established by DSC (*vide supra*). The DMA traces of **azo-PU** and **ref-PU** (Figure 2c, Supporting Information, Figure S26) show the typical features of a phase separated

segmented polyurethane, with a T_g of -41 °C and a rubbery plateau that extends up to the failure temperature of ca. 150 °C (**azo-PU**) and 180 °C (**ref-PU**). The T_g of the **azo-PU** is slightly broader than that of the **ref-PU**, and therefore the azo motif causes a slight increase of *E*' in the region between T_g and ca. 100 °C, where *E*' drops below that of the **ref-PU.** The slanted nature of the rubbery plateau, the lower failure temperature of **azo-PU** vis a vis **ref-PU**, and the thermal data discussed above, suggest that the softening and mechanical failure of **azo-PU** at higher temperature is indeed related to the thermal dissociation of the azo motif. Overall the PAs are stiffer than the PUs, both in the glassy as well as in the rubbery state (Supporting Information, Figures S25 and S26). Both materials are rubbery at room temperature, but while the PUs presented a very high toughness (*vide infra*), it was impossible to perform any stress-strain measurement with the PAs, presumably due to their limited molecular weight.

Controlled degradation of azo-containing polyamide

The thermally induced decomposition behavior of **azo-PA** and **ref-PA** was first probed in solution. Thus, the polymers were dissolved at a concentration of 2.5 mg/mL under ambient conditions in either acetonitrile (MeCN) or carbon tetrachloride (CCl_4), which were chosen with the objective to compare the dissociation behavior in solvents of inert nature (MeCN) and high chain transfer constant (CCl_4).[26] The solutions were rapidly heated to 140 °C (i.e., the decomposition temperature identified by TGA and DSC, *vide supra*) using pressure-resistant vials and a microwave synthesizer, maintained at this temperature for 5 min, and then rapidly cooled to ambient temperature. Changes to the molecular weight and the dispersity were analyzed by SEC (Figure 3, Table 2).

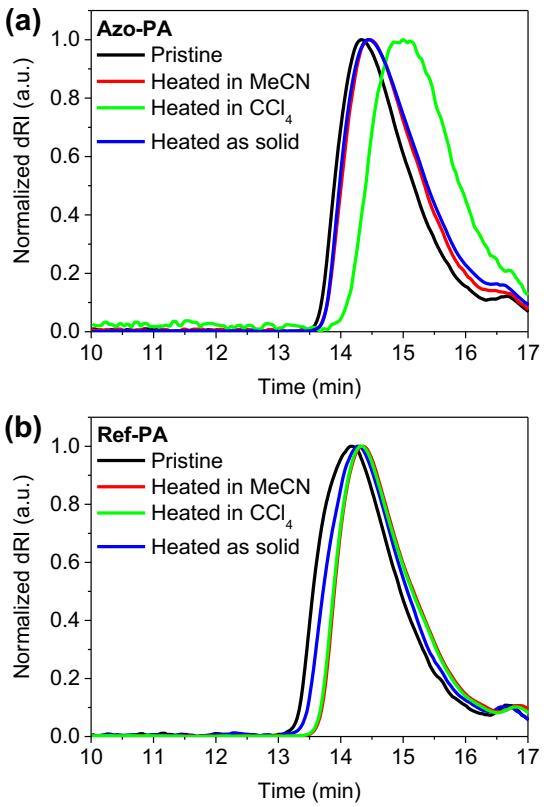

Figure 3. Size exclusion chromatography (SEC) traces of (a) the azo-containing polyamide **azo-PA** and (b) the azo-free reference **ref-PA** in the pristine state (black lines), and after heat treatment (5 min at 140 °C) of 2.5 mg/mL solutions in MeCN (red lines), CCl_4 (green lines) or in the solid state (blue lines).

Interestingly, in MeCN, only a minor reduction of M_n was observed by SEC for both **azo-PA** and **ref-PA** (Figure 3, Table 2), which we interpret as the result of unspecific thermal degradation, perhaps hydrolysis of the amide groups by trace amounts of water present. In the case of **azo-PA**, the azo motifs are certainly cleaved by the treatment as confirmed by the above-discussed thermal data, but the SEC data suggest that the macroradicals formed instantly recombine after N_2 release, so that the molecular weight is not reduced. This behavior was already reported by Moore and coworkers for a poly(ethylene glycol) comprising the same azo

motif used here in the center of the polymer chain, upon thermal treatment in the same solvent.[25] Speculating that such recombination could be stifled by way of radical transfer to the solvent, the thermal degradation experiment was repeated, but CCl_4 was employed as the solvent. While the behavior of the azo-free **ref-PA** remained, as expected, unchanged, a pronounced reduction of M_n from 23,400 to 11,200 g/mol was observed in the case of the **azo-PA**, as a result of the thermally induced cleavage of the azo motif and abstraction of the radicals from the polymer fragments. Thus, conducting the thermally induced degradation in the presence of a chain transfer agent has a significant influence on the fate of the polymer radicals formed in the process, and permits suppressing their instant recombination. Generally, $Đ$ increased only slightly, except in CCl_4, where an increase from 1.41 to 1.96 was observed.

Table 2. Molecular weights of azo-PA and ref-PA in their pristine state and after heating under different conditions.

	Azo-PA			**Ref-PA**		
	M_n[a] (g/mol)	M_w[a] (g/mol)	$Đ$[a]	M_n[a] (g/mol)	M_w[a] (g/mol)	$Đ$[a]
Pristine	23,400	33,000	1.41	24,700	41,300	1.67
Heated in MeCN	18,900	31,100	1.65	19,600	29,500	1.51
Heated in CCl_4	11,200	21,900	1.96	20,000	30,000	1.50
Heated in solid state	20,100	30,000	1.49	21,800	35,300	1.62

[a]Determined by size exclusion chromatography (SEC). The samples were dried before they were heated for 5 min at 140 °C in acetonitrile (MeCN), tetrachloromethane (CCl_4), or the solid state. The concentration of the polymers in the solutions was 2.5 mg/mL.

We also explored the thermal degradation of **azo-PA** and **ref-PA** in the solid state (140 °C for 5 min), but not surprisingly the results (Figure 3, Table 2) mirror the behavior observed for the MeCN solution. To confirm that the thermal treatment in absence of a chain transfer agent (i.e. in

MeCN solution and in the solid state) indeed triggered decomposition of the azo motif under N_2 release and recombination of the resulting radicals, we compared the ^{1}H NMR spectra of heated (in the solid state at 140 °C for 5 min and then dissolved in $CDCl_3$) and pristine samples (Supporting Information, Figure S5a, b), and observed changes in the characteristic signals of the methylene and methyl groups introduced by the azo moiety, i.e. around 2.46-2.25 (m, 4H, CH_2, obstructed) and 1.70 ppm (d, 6H, CH_3). Furthermore, elemental analyses showed a significant reduction of the nitrogen content after heating (140 °C for 5 min) the **azo-PA** in solid state (Supporting Information). Thus, the thermally induced degradation of **azo-PA** strongly depends on and can be controlled by the nature of the environment; while heating invariably triggers the release of N_2, the choice of the immediate environment is crucial, as recombination effects can be moderated via chain transfer to the latter. We speculate that a similar mechanism can also be exploited in the solid state, although this was not further probed in the present study.

Controlled degradation of azo-containing polyurethane

Since neither **azo-PU** nor **ref-PU** are soluble in MeCN or CCl_4, the thermal degradation of these polymers was studied in tetrahydrofuran (THF) using pressure-withstanding vials and a microwave synthesizer. Based on the TGA and DSC data samples were heated to 150 °C for 5 min, but otherwise the same conditions as used for the PAs were applied. While the molecular weight of **ref-PU** was not affected at all by this treatment (Figure 4, Table 3), the M_n of the **azo-PU** was reduced from 49,300 to 23,100 g/mol**,** indicating the cleavage of the azo motifs and the absence of substantial recombination of the macroradicals formed. An even more pronounced reduction to 16,400 g/mol was observed when **azo-PU** was heated in the solid state. Other conditions (temperature, time) were explored for both solution and solid state studies (Suppor-

ting Information, Figures S27 and S29) and the results indicate that treatment at 150 °C for 5 min is an effective treatment for the decomposition of **azo-PU**. Heating the **azo-PU** at 160 °C for 5

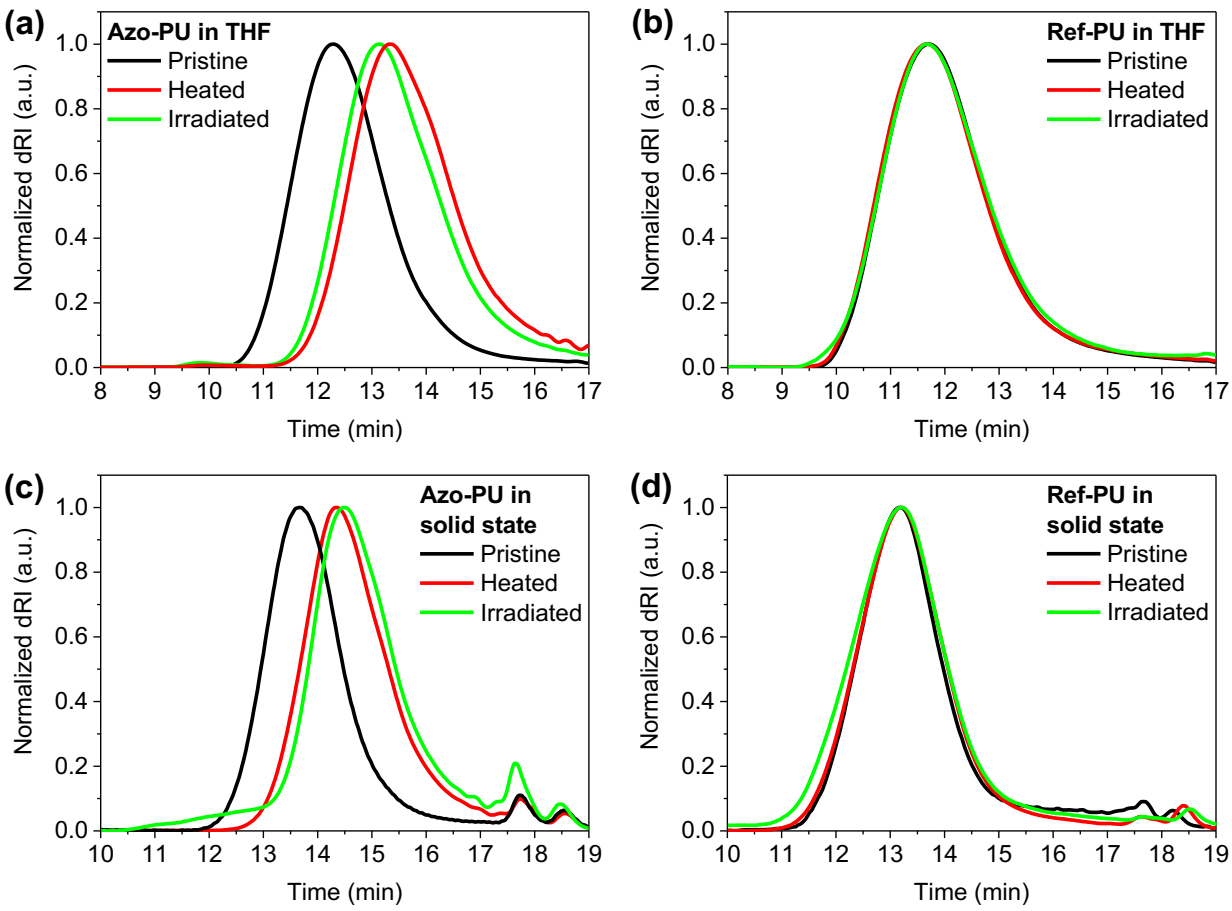

Figure 4. Size exclusion chromatography (SEC) traces of (a, c) the azo-containing polyurethane **azo-PU** and (b, d) the azo-free reference **ref-PU** in the pristine state (black lines) and after heat treatment (5 min at 150 °C, red lines) or exposure to UV light (320-390 nm, 600 mW/cm^2, green lines) in (a, b) THF solution (2.5 mg/mL, 15 sec) or (c, d) the solid state (30 sec).

min gave lower M_n in solution but the decomposition was fast enough in solid state that bubbles stayed trapped within the material because N_2 formed very rapidly. These results reflect that the degradation of the **azo-PU** is less substantially moderated by the environment than that of the **azo-PA** studied here. Indeed, the specific azo motif employed in the **azo-PA**, featuring methyl,

nitrile, and methylene groups α to the N_2 bridge, decomposes under formation of radicals that are substantially less reactive than those formed by decomposition of the motif used in **azo-PU**, where stabilization is provided only through an amide and two methyl groups.[27,28] Experimental evidence has been provided by photolysis reactions of model azo compounds that revealed a higher quantum efficiency for a molecule similar to **2** than for an analogous of **1.**[29] The slightly lower M_n value observed when **azo-PU** was heated in the solid state (vis a vis the THF solution) seems to indicate that more radical recombinations occur in solution than in the solid state (*vide infra*), possibly because the lower translational mobility in the latter facilitates proton abstraction, which is less favored in solution.

Table 3. Molecular weights of azo-PU and ref-PU in their pristine state and after heating or exposure to UV light.

	M_n[a] (g/mol)	
	Azo-PU	**Ref-PU**
Pristine	49,300	93,600
Heated in THF	23,100	94,400
Irradiated in THF	23,700	95,400
Heated in the solid state	16,400	91,800
Irradiated in the solid state	15,200	93,400

[a]Determined by size exclusion chromatography (SEC). All samples were dried before any treatment (heating for 5 min at 150 °C or exposure to UV light at 600 mW/cm^2 for 15 sec in solution and 30 sec in the solid state). The concentration of the polymers in THF was 2.5 mg/mL.

As mentioned above, many azo compounds not only function as thermal initiators, but can also be used as photoinitiators,[27] as they display an optical absorption band in the visible or the UV A

range that permits optical excitation with readily accessible light sources. Indeed, this mechanism has been reported for 2,2'-azobis[2-methyl-N-(2-hydroxyethyl)propionamide] (**2**),[34,35] which displays an absorption band that stretches from 420 to 300 nm and displays a maximum around 370 nm (in water, 0.028 M, Supporting Information, Figure S32). We speculated that this characteristic could be exploited for the controlled degradation of **azo-PU** using UV or visible light. Despite the low content of the azo-moiety and the low extinction coefficient of the monomer **2** (12.32 $L \cdot mol^{-1} \cdot cm^{-1}$), the absorption spectrum of **azo-PU** clearly shows the characteristic shoulder associated with this motif (Supporting Information, Figure S35). Dilute (2.5 mg/mL) solutions of the two PUs in THF were exposed to UV light using a high power lamp (320-390 nm, 600 mW/cm^2, 15 sec) under stirring. Gratifyingly, SEC analysis indicates that the effects of the irradiation are virtually identical to those observed upon heating: while the molecular weight of the **ref-PU** remained unchanged, the M_n of the **azo-PU** was reduced from 49,300 to 23,700 g/mol**.** Variation of the excitation time between 7.5 and 60 sec (Supporting Information, Figure S33) shows that the light-induced dissociation is (under the conditions employed here) indeed complete in as little as 15 sec. The optically induced molecular weight reduction of **azo-PU** was comparable when the experiment was conducted in THF solution containing 5 drops of CCl_4 (Supporting Information, Figure S33), suggesting that the presence of an auxiliary chain transfer agent is not needed to suppress dimerization of the macroradicals formed.

One of the attractive features of using light as a stimulus is that it can readily be applied, if desired also in a spatially resolved fashion, to solid specimens. Thus, films of the two polyurethanes were irradiated with UV light (320-390 nm, 600 mW/cm^2 for 30 sec) and SEC analyses were subsequently performed (Figure 4c and d, Table 3). Note that the absorption associated

with the azo-motif is small and it decreases upon UV exposure so that cleavage is likely to be homogeneous throughout the sample (Supporting Information, Figure S35). Also in this case, the molecular weight of **ref-PU** was not affected by the treatment with UV light, whereas the M_n of the **azo-PU** was reduced from 49,300 to 15,200 g/mol**.** As in the case of the thermal treatment of the **azo-PU**, the molecular weight reduction was slightly more pronounced in the solid state than in solution, suggesting that more recombination of the macroradicals may occur in the latter (*vide supra*). We also subjected the **azo-PA** to UV light irradiation, but as expected on the basis of the results obtained after thermal treatment (*vide supra*), the molecular weight did not decrease (Supporting Information, Figures S41 and S42).

Although the UV-Vis spectra of **2** and the **azo-PU** (Supporting Information, Figures S32 and S35) show only little absorption above 400 nm, we explored the response of thin films upon irradiation with visible light in the range of 390-500 nm using the same lamp at the same power density (600 mW/cm^2). Also, in this case, a M_n decrease was observed for the **azo-PU** while the **ref-PU** was not altered (Supporting Information, Figures S47-S51). Even if a slightly longer (60 vs. 30 sec) irradiation time was required to reach a similar M_n as afforded by exposure to UV light, the **azo-PU** is clearly responsive to short-wavelength visible light. An IR camera was used to monitor the temperature of the films during the light irradiation processes, and the temperature-time diagrams (Supporting Information, Figures S38, S40, S49 and S51) reveal only a very small temperature increase (ca. 10 °C and 3 °C upon exposure to UV and visible light, respectively), indicating that the process is purely optically engendered. Only a minor increase of $Đ$ was observed in all cases, unless the samples were heated or irradiated with UV light for longer periods.

In the case of the **azo-PU**, a comparison of the M_n values before (49,300 g/mol) and after (15,700-30,900 g/mol) optical or thermal treatment in the solid state and the average number of azo moieties incorporated into the polymer backbone (8-9) suggests that not all azo motifs lead to chain cleavage. Assuming a statistical incorporation of the azo moieties and 100% cleavage, the theoretical M_n value that should be obtained after complete cleavage would be ca. 5,800 g/mol. To investigate this discrepancy, an ^{1}H NMR study was conducted. The characteristic signals of pristine and heated (solid state, 150 °C for 5 min) **azo-PU** samples were monitored and compared. An analysis of these signals reveals that: (i) a portion of the azo moieties dissociated and caused cleavage of the backbone, (ii) another portion of the azo moieties dissociated but the radicals recombined, and (iii) a portion of the azo moieties did not react. The diagnostic signals that were monitored include a singlet at 1.33 ppm corresponding to methyl protons of the azo moiety in the pristine material (Supporting Information, Figures S13a, c), a septet at 2.27 ppm, in the heated material, which is interpreted as a proton α to the two methyl groups, meaning that proton abstraction occurred. This is supported by the presence of a coupling partner at 1.05 ppm (doublet, methyl protons). Also, a singlet at 1.18 ppm in the heated material corresponds to the methyl groups of the recombined species. Analysis of the related integrals suggests that heating of 5 min at 150 °C affords approximate 37% of the cleaved product and 28% of the recombined species, whereas 35% of the azo motifs remain intact. These results correlate with the calculated assumption that 8-9 azo moieties are present per chain (*vide supra*) and explain the ca. threefold M_n reduction observed after treatment. In the case of a longer heating (solid state, 150 °C for 30 min), the signal at 1.33 ppm completely disappeared, meaning that all azo moieties decomposed and the radicals either reacted or recombined (Supporting Information, Figures S13b, c). The ratio between the integrals of the reacted (1.05 ppm) and recombined (1.18 ppm) species

remained the same at ca. 1.3-1.4. As a result of the complete decomposition of the azo motifs, the M_n decrease was slightly more pronounced (Supporting Information, Figure S31). Moreover, this observation confirms that the complete N_2 release, as exposed by TGA, i.e. ca. 1 wt% (*vide supra*), can also be reached by applying an appropriate short treatment. The ^{1}H NMR spectra of the pristine and heated (solid state, 150 °C for 5 min) **ref-PU** were identical and therefore support the absence of any degradation (Supporting Information, Figures S15-S18).

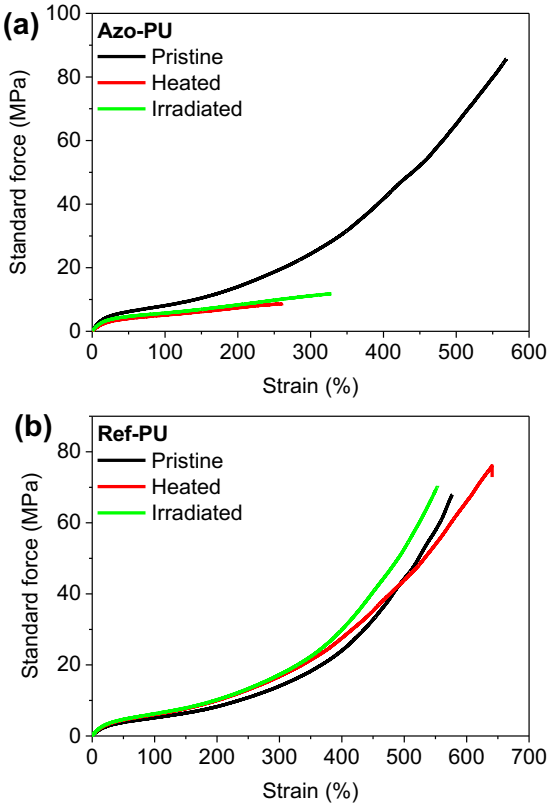

Figure 5. Representative stress-strain curves of films of the (a) azo-containing **azo-PU** and (b) the azo-free reference **ref-PU** in the pristine state (black lines), and after heat treatment (5 min at 150 °C, red lines) or exposure to UV light (320-390 nm, 600 mW/cm^2, 30 sec, green lines). The film thickness was in all cases 120 μm.

Assuming that the significant M_n decrease induced by heat and exposure to UV light would exert a significant influence on the material mechanical properties of the **azo-PU**, stress-strain measurements of pristine and heat or light-treated **azo-PU** and **ref-PU** were performed (Figure 5). The heat treatment was applied prior to cutting whereas the light irradiation was locally performed after, and limited to the central part of the specimen (Supporting Information, Figure S43a). The light irradiation had no influence on the visual appearance of the sample (Supporting Information, Figure S43b) and on its thickness (i.e. 120 μm). Again, temperature-time diagrams were recorded to confirm that the temperature increase was negligible (Supporting Information, Figures S44-S45). The mechanical properties of the pristine, heat-treated, and light-treated **ref-PU** samples are virtually identical (Figure 5b); the stress-strain curves are characteristic of a phase-segregated thermoplastic elastomer, with an elongation at break (ε_R) between 563 ± 18 and 606 ± 70% and a stress at break (σ_R) of 64 ± 19 - 75 ± 5 MPa (Supporting Information, Table S46). The characteristics of the pristine **azo-PU** are also similar, with a ε_R of 556 ± 25% and a σ_R of 81 ± 9 MPa. By contrast, the heated and UV-exposed specimens showed a substantial reduction of ε_R to 270 ± 35% and 333 ± 6%, respectively, and of σ_R to 9 ± 1 MPa and 13 ± 1 MPa, respectively. Thus, while the mechanical properties are significantly changed, the degraded materials retain mechanical integrity and are merely weakened. This is confirmed by analyzing the Young's modulus (E) values, which in the case of the **azo-PU** were reduced from 41 ± 1 MPa (pristine) to 24 ± 1 MPa upon heating and 35 ± 1 MPa upon light-treatment (Supporting Information, Table S46). The **ref-PU** has a slightly a lower stiffness than the **azo-PU**, as was shown by DMA (*vide supra*), and its E hardly changed from 19 ± 1 MPa upon heating (to 22 ± 1 MPa) or UV light treatment (24 ± 1 MPa). The fact that that the irradiated samples exhibited slightly higher ε_R, σ_R, and E than the heated materials seem to contrast the fact that lower

molecular weights were observed for the irradiated samples (*vide supra*) but the small difference may be related to the fact that the UV light was locally applied (on ca. 15 mm of the 30 mm of the measured part), whereas the heating was applied homogeneously to the entire specimens.

As mentioned above, one attractive feature of using light as a stimulus is that it can be applied locally and in a spatially resolved manner, for example by using a photomask that creates a specific pattern or gradient. This was explored by applying a simple mask that allowed degrading selected areas of a rectangular film of **azo-PU** upon exposure to UV light, while others were left in the pristine state (Figure 6, zones 2 and 4 were irradiated with 320-390 nm UV light at 600 mW/cm^2 for 30 sec). The images shown in Figure 6 show strikingly that such treatment permits the creation of objects with locally varying mechanical properties, in which mechanical deformation leads to inhomogeneous deformation. Indeed, the relative extension of the pristine zones (1 and 3) is much less pronounced than that of the degraded zones (2 and 4), which is in accordance with the different deformation behaviors established for the pristine and degraded **azo-PU** (Figure 5).

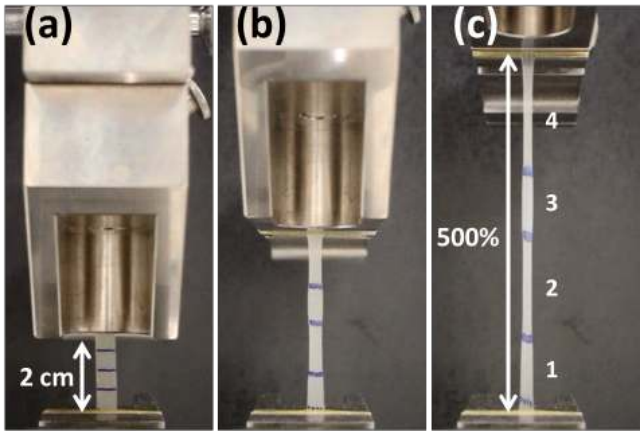

Figure 6. Images showing a photopatterned **azo-PU** film (a) before, (b) during, and (c) after being subjected to an overall elongation of 500%. Zones 2 and 4 had been irradiated with 320-

390 nm UV light at 600 mW/cm^2 for 30 sec, whereas zones 1 and 3 had been covered with a photomask and remained unexposed.

CONCLUSIONS

In summary, we have shown that azo moieties can not only be used as radical polymerization initiators but also as thermally and optically addressable motifs that permit the design of polymers whose molecular weight can be reduced on demand. We presented here novel types of azo-containing polymers that were prepared via straightforward step-growth polymerization reactions; we focused on simple polyamides and polyurethanes, but of course the framework presented here is readily applicable to other polymers, provided that the reaction can be conducted at a sufficiently low temperature. Our systematic study revealed that the stimuli-induced degradation of the molecular weight is not only possible, but that it depends strongly on the nature of the polymer backbone, the state of matter, and, in solution, also on the nature of the solvent. Most of all is the azo moiety design of importance. Indeed, the more stable macroradicals formed in the case of the azo-containing polyamide (**azo-PA**) required the presence of a chain-transfer agent so that recombination be suppressed. This was shown in solution where CCl_4 was used as solvent and in which dissolved **azo-PA** was rapidly heated and exposed a MW decrease. Moreover, the reactive radicals originating from the azo-containing polyurethane (**azo-PU**) exhibited the tendency to react further instead of recombining. We demonstrated that the thermal or optical treatment applied to the **azo-PU** can exert a significant influence on the material's mechanical properties, in the form of pronounced elongation and stress at break reductions. The controlled degradation of the polymer in well-defined areas can readily be achieved via photopatterning, and this approach was shown to be useful to produce

solid structures with graded mechanical properties. We speculate that materials such as the ones presented here may be useful for debonding-on-demand adhesives, recyclable composite materials, and mechanically graded connectors. The concept should also be useful to create gels with programmable mechanical properties, which are useful to influence the development of cultured cells.

ASSOCIATED CONTENT

Supporting Information. A supporting information containing FT-IR, NMR, EA, DMA, TGA, DSC, SEC analyses and details about the heating and light irradiation experiments is available free of charge via the Internet at http://pubs.acs.org.

AUTHOR INFORMATION

Corresponding Author

*E-mail: christoph.weder@unifr.ch (C.W.).

Notes

The authors declare no competing financial interest.

ACKNOWLEDGMENTS

The authors thank Prof. Bernd Giese (University of Fribourg) for stimulating discussions. The authors acknowledge funding from the European Research Council (Grant ERC-2011-AdG 291490-MERESPO) and the Adolphe Merkle Foundation. This work was also partially

supported by the National Center of Competence in Research (NCCR) Bio-Inspired Materials, a research instrument of the Swiss National Science Foundation.

REFERENCES

(1) Delplace, V.; Nicolas, J. Degradable vinyl polymers for biomedical applications. *Nat. Chem.* **2015,** *7*, 771-784.

(2) Heinzmann, C.; Weder, C.; de Espinosa, L. M. Supramolecular polymer adhesives: advanced materials inspired by nature. *Chem. Soc. Rev.* **2016,** *45*, 342-358.

(3) Huu, V. A. N.; Luo, J.; Zhu, J.; Zhu, J.; Patel, S.; Boone, A.; Mahmoud, E.; McFearin, C.; Olejniczak, J.; Lux, C. D.; Lux, J.; Fomina, N.; Huynh, M.; Zhang, K.; Almutairi, A. Light-responsive nanoparticle depot to control release of a small molecule angiogenesis inhibitor in the posterior segment of the eye. *J. Controlled Release* **2015,** *203*, 39-39.

(4) Mohapatra, H.; Kim, H.; Phillips, S. T. Stimuli-Responsive Polymer Film that Autonomously Translates a Molecular Detection Event into a Macroscopic Change in Its Optical Properties via a Continuous, Thiol-Mediated Self-Propagating Reaction. *J. Am. Chem. Soc.* **2015,** *137*, 12498-12501.

(5) Stuart, M. A. C.; Huck, W. T. S.; Genzer, J.; Muller, M.; Ober, C.; Stamm, M.; Sukhorukov, G. B.; Szleifer, I.; Tsukruk, V. V.; Urban, M.; Winnik, F.; Zauscher, S.; Luzinov, I.; Minko, S. Emerging applications of stimuli-responsive polymer materials. *Nat. Mater.* **2010,** *9*, 101-113.

(6) Roy, D.; Cambre, J. N.; Sumerlin, B. S. Future perspectives and recent advances in stimuli-responsive materials. *Prog. Polym. Sci.* **2010,** *35*, 278-301.

(7) Yoshida, T.; Lai, T. C.; Kwon, G. S.; Sako, K. pH- and ion-sensitive polymers for drug delivery. *Expert Opinion on Drug Delivery* **2013,** *10*, 1497-1513.

(8) Peterson, G. I.; Larsen, M. B.; Boydston, A. J. Controlled Depolymerization: Stimuli-Responsive Self-Immolative Polymers. *Macromolecules* **2012,** *45*, 7317-7328.

(9) Roy, D.; Brooks, W. L. A.; Sumerlin, B. S. New directions in thermoresponsive polymers. *Chem. Soc. Rev.* **2013,** *42*, 7214-7243.

(10) Schattling, P.; Jochum, F. D.; Theato, P. Multi-stimuli responsive polymers – the all-in-one talents. *Polym. Chem.* **2014,** *5*, 25-36.

(11) Seo, W.; Phillips, S. T. Patterned Plastics That Change Physical Structure in Response to Applied Chemical Signals. *J. Am. Chem. Soc.* **2010,** *132*, 9234-9235.

(12) Lee, M. E.; Gungor, E.; Armani, A. M. Photocleavage of Poly(methyl acrylate) with Centrally Located o-Nitrobenzyl Moiety: Influence of Environment on Kinetics. *Macromolecules* **2015,** *48*, 8746-8751.

(13) Yeung, K.; Kim, H.; Mohapatra, H.; Phillips, S. T. Surface-Accessible Detection Units in Self-Immolative Polymers Enable Translation of Selective Molecular Detection Events into Amplified Responses in Macroscopic, Solid-State Plastics. *J. Am. Chem. Soc.* **2015,** *137*, 5324-5327.

(14) Neradovic, D.; van Nostrum, C. F.; Hennink, W. E. Thermoresponsive polymeric micelles with controlled instability based on hydrolytically sensitive N-isopropylacrylamide copolymers. *Macromolecules* **2001,** *34*, 7589-7591.

(15) Lo, C. L.; Lin, S. J.; Tsai, H. C.; Chan, W. H.; Tsai, C. H.; Cheng, C. H. D.; Hsiue, G. H. Mixed micelle systems formed from critical micelle concentration and temperature-sensitive diblock copolymers for doxorubicin delivery. *Biomaterials* **2009,** *30*, 3961-3970.

(16) Kot, E.; Bismarck, A. Polyacrylamide Containing Weak Temperature Labile Azo Links in the Polymer Backbone. *Macromolecules* **2010,** *43*, 6469-6475.

(17) Haseloh, S.; van der Schoot, P.; Zentel, R. Control of mesogen configuration in colloids of liquid crystalline polymers. *Soft Matter* **2010,** *6*, 4112-4119.

(18) Agarwal, S.; Grabe, N. Use of Reactive and Functional Hydrophobes (Hydrophobins) in the Miniemulsion Polymerization of Styrene and Methyl Methacrylate. *Macromol. Chem. Phys.* **2011,** *212*, 391-400.

(19) Grabe, N.; Zhang, Y.; Agarwal, S. Degradable Elastomeric Block Copolymers Based on Polycaprolactone by Free-Radical Chemistry. *Macromol. Chem. Phys.* **2011,** *212*, 1327-1334.

(20) Ueda, A.; Shiozu, Y.; Hidaka, Y.; Nagai, S. Studies on Block Copolymers Derived from Azobiscyanopentanoic Acid. *Kobunshi Ronbunshu* **1976,** *33*, 131-140.

(21) Ahn, T. O.; Kim, J. H.; Lee, J. C.; Jeong, H. M.; Park, J.-Y. Polyarylate–polystyrene block copolymer from macro-azoinitiator: Synthesis and its thermal properties. *J. Polym. Sci., Part A: Polym. Chem.* **1993,** *31*, 435-441.

(22) Hickenboth, C. R.; Rule, J. D.; Moore, J. S. Preparation of enediyne-crosslinked networks and their reactivity under thermal and mechanical conditions. *Tetrahedron* **2008,** *64*, 8435-8448.

(23) Riedinger, A.; Guardia, P.; Curcio, A.; Garcia, M. A.; Cingolani, R.; Manna, L.; Pellegrino, T. Subnanometer Local Temperature Probing and Remotely Controlled Drug Release Based on Azo-Functionalized Iron Oxide Nanoparticles. *Nano Lett.* **2013,** *13*, 2399-2406.

(24) Saint-Cricq, P.; Deshayes, S.; Zink, J. I.; Kasko, A. M. Magnetic field activated drug delivery using thermodegradable azo-functionalised PEG-coated core-shell mesoporous silica nanoparticles. *Nanoscale* **2015,** *7*, 13168-13172.

(25) Berkowski, K. L.; Potisek, S. L.; Hickenboth, C. R.; Moore, J. S. Ultrasound-induced site-specific cleavage of azo-functionalized poly(ethylene glycol). *Macromolecules* **2005,** *38*, 8975-8978.

(26) Brandrup, J.; Immergut, E. H.; Grulke, E. A., *Polymer handbook*, 4th ed.; Wiley: New York; Chichester, 2004; p 2317.

(27) Oster, G.; Yang, N. L. Photopolymerization of Vinyl Monomers. *Chem. Rev.* **1968,** *68*, 125-151.

(28) Coote, M. L.; Lin, C. Y.; Zipse, H., The Stability of Carbon-Centered Radicals. In *Carbon-Centered Free Radicals and Radical Cations*, Forbes, M. D. E., Ed. John Wiley & Sons, Inc.: Hoboken, 2010; pp 83-104.

(29) Calvert, J. G.; Pitts, J. N., *Photochemistry*, Wiley: New York, 1966; p 899.

(30) Engel, P. S. Mechanism of the thermal and photochemical decomposition of azoalkanes. *Chem. Rev.* **1980,** *80*, 99-150.

(31) Weder, C.; Neuenschwander, P.; Suter, U. W.; Pretre, P.; Kaatz, P.; Gunter, P. New Polyamides with Large Second-Order Nonlinear Optical Properties. *Macromolecules* **1994,** *27*, 2181-2186.

(32) Phillips, R. E.; Soulen, R. L. Propylene Oxide Addition to Hydrochloric Acid - A Textbook Error. *J. Chem. Educ.* **1995,** *72*, 624-625.

(33) Crenshaw, B. R.; Weder, C. Self-assessing photoluminescent polyurethanes. *Macromolecules* **2006,** *39*, 9581-9589.

(34) Yamanaka, J.; Murai, M.; Yamada, H.; Ozaki, H.; Uchida, F.; Sawada, T.; Tomitama, A.; Ito, K.; Takiguchi, Y.; Taira, H. JP2006182833A, July 13, 2006.

(35) Takeda, T.; Goto, T.; Mori, Y. JP2003212917A, April 27, 2003.

TOC Entry

Azo-Containing Polymers with Degradation On-Demand Feature

Mathieu A. Ayer[1], Yoan C. Simon[1,2], Christoph Weder[1]*

[1]Adolphe Merkle Institute, University of Fribourg, Chemin des Verdiers 4, 1700 Fribourg, Switzerland

[2]School of Polymers and High Performance Materials, The University of Southern Mississippi, 118 College Dr., Hattiesburg MS 39406, USA

*E-mail: christoph.weder@unifr.ch (C.W.).